Desorption dynamics of deuterium molecules from the Si(100)-(3×1) dideuteride surface

T. Niida, H. Tsurumaki, and A. Namiki[a)]
Department of Electrical Engineering, Kyushu Institute of Technology, Kitakyushu 804-8550, Japan

(Received 25 July 2005; accepted 3 November 2005; published online 11 January 2006)

We measured polar angle (θ)-resolved time-of-flight spectra of D_2 molecules desorbing from the Si(100)-(3×1) dideuteride surface. The desorbing D_2 molecules exhibit a considerable translational heating with mean desorption kinetic energies of ≃0.25 eV, which is mostly independent of the desorption angles for $0° \leqslant \theta \leqslant 30°$. The observed desorption dynamics of deuterium was discussed along the principle of detailed balance to predict their adsorption dynamics onto the monohydride Si surface. © *2006 American Institute of Physics*. [DOI: 10.1063/1.2141953]

I. INTRODUCTION

Adsorption and desorption of hydrogen molecules on Si surfaces are of great relevance not only to semiconductor device technology but also to basic science in the field of gas-surface dynamics. Due to strong, highly directional covalent bonding, adsorption/desorption of hydrogen on the Si surfaces is accompanied by a considerable displacement of substrate atoms. Yet, dynamics of the substrate atoms during the reaction is not able to be measured directly with any sophisticated instruments such as a scanning tunneling microscope (STM). Desorbed molecules may convey a message of such unmeasurable Si dynamics. The recent experiments on Si(100)-(2×1) monohydride surfaces for hydrogen coverage (θ_H) below 1.0 ML have demonstrated that the desorption dynamics of hydrogen (deuterium)[1,2] is related to the adsorption dynamics of hydrogen[3,4] via detailed balance. This implies that the desorption proceeds along a reversed process of the adsorption reaction, overcoming the same barriers for adsorption. Vibrational degrees of freedom of substrate Si atoms play an essential role to the barriers for adsorption, since it has been suggested that as much as one-third of ~1.0 eV barriers for adsorption is disposed to the Si lattice while desorbing molecules receive average translational energies of only 0.35–0.4 eV from it.[1] One should recall that such energetic desorption overcoming the high adsorption barriers takes place for $\theta_H \leqslant 0.8$ ML, but a barrierless pathway or the so-called 4H pathway[5,6] is accessed only for high coverage region around 1.0 ML.[7]

Desorption of hydrogen also takes place on a (3×1) dihydride phase for $\theta_H > 1.0$ ML with a maximum desorption rate at 620–650 K in a temperature-programmed desorption (TPD). The early experiments showed up the desorption feature characterized with a second-order rate law and desorption energy barrier of 1.9–2.0 eV,[8,9] which is much lower than the desorption barriers (~2.5 eV) on the (2×1) monohydride phases.[9,10] The observed second-order rate law in the dihydride coverage suggests that the desorption occurs from two neighboring dihydrides (SiH_2), which could be prepared by site exchange between doubly occupied Si dimer HSi–SiH and SiH_2 via an isomerization reaction,[11] leaving behind a doubly occupied Si dimer,[12]

$$2SiH_2 \rightarrow HSi - SiH + H_2. \quad (1)$$

Recently, evidence of the above desorption from two adjacent dihydrides arranged via isomerization reaction was given in the STM images.[13] They showed that molecules can be desorbed from a local (1×1) dihydride patch, but cannot be desorbed from the isolated dihydrides.

Internal state distributions of hydrogen molecules desorbing from the (3×1) dihydride phase were measured by Kolasinski and co-workers who employed a resonance-enhanced multiphoton ionization (REMPI) method, showing rotationally cold but vibrationally hot molecular desorption.[14,15] They argued that the desorption dynamics from the dihydride phase is quite similar to those from the monohydride phase. Kolasinski *et al.*[16] further measured time-of-flight distributions of D_2 molecules desorbed by a pulsed-laser desorption (PLD), and found complete accommodation with the surface, similarly to the case of desorption from the monohydride phase. The similarity of the desorption dynamics led them to such a conclusion that the transition state for desorption is the same on the two phases.

Under such circumstance the energetics relevant to the dihydride reactions were calculated based on a cluster model[11,17] and on a slab model.[18–20] Taking the desorption reaction occurring from two adjacent dihydrides or Eq. (1) into consideration, the slab calculations were done for the (1×1) dihydride phase. To reduce sterically repulsive interaction energy between neighboring H atoms, a canted Si dihydride structure was favored rather than a symmetric one. The *ab initio* calculations predicted that the change of enthalpy upon desorption is slightly negative[19] or only slightly positive;[17] hence the barriers for adsorption and desorption could be more or less the same, ~2.0 eV, which is approximately double the adsorption barrier on the monohydride phase. Vittadini and Selloni[19] theoretically revealed that the lattice distortion energy at the transition state is as high as 1.65 eV, sharing the most part of the energy barrier for adsorption. Thus the lack of translational heating found in the

[a)]Electronic mail: namiki@ele.kyutech.ac.jp

PLD experiments could be rationalized. Such a high barrier for adsorption was considered to be a result of energy cost in breaking a HSi–SiH dimer bond.[19]

However, the lack of translational heating observed in the PLD experiments[16] seems to contradict the vibrational heating observed in the REMPI/TPD experiments[14,15] since the molecular vibration and translation are generally coupled to each other, giving rise to heating the both motions.[21] In the case of the PLD experiments, because of a too high heating rate ($\sim 10^{10}$ K/s) equilibrium desorptions may not be automatically assured. Furthermore, actual desorption temperatures could not be directly measured. This would lead to some ambiguities whether desorption is induced from dihydride units or from monohydride units via the 4H pathway.

In this paper we report angle-resolved time-of-flight (TOF) distributions of D_2 molecules desorbed in TPD from the Si(100)-(3×1) dideuteride surfaces. Considerable translational heating is found, mostly independent of the desorption angle θ. Applying detailed balance the observed desorption dynamics of D_2 molecules from the dideuteride phases is interpreted in terms of predicted adsorption dynamics of D_2 on the monohydride surface.

II. EXPERIMENT

Experimental details have been reported previously.[1] Here we describe only the essence of experiments. Angle-resolved TOF distributions were measured using a cross-correlation method. The net flight distance (L) from the quasirandom chopper to an ionizer of a quadrupole mass spectrometer (QMS) is 33.2 cm long. Molecules desorbed in a reaction chamber pass through four-fixed apertures in four differentially pumped chambers before being detected with the QMS. This ensures preferential detection of highly collimated components. Effusive gas which has not passed through rotating quasirandom slits contributes simply as a white background, being then distinguished from TOF components. The desorption polar angles were changed by means of sample rotation. Generally, 100 TPD spectral scans with a 6 K/s heating rate for 400 K$\leqslant T_s \leqslant$1150 K were repeated to obtain one TOF spectrum. After each TPD spectral scan the sample was cooled down with a cooling rate less than 1.0 K/s to avoid roughing the surface. The initial D coverage was about 1.33 ML and thus the surface was saturated with (3×1) dihydride phases. Data acquisition with a multichannel scaler (MCS) was manually gated by monitoring each TPD spectral scan on a scope of the QMS, as drawn in the inset of Fig. 1 This allowed us to count molecules desorbed along the β_2-TPD path from the (3×1) phase.

III. RESULTS AND DISCUSSION

Figure 1 shows the D_2 TOF density distribution measured for $\theta=20°$. Comparing with the 620 K Maxwellian curve, one should note that the TOF curve is heated more than expected at equilibrium with the surface. Thus the result is not agreeable with the result of Kolasinski *et al.* in which the desorbing molecules exhibited the nonheated translational motions.[16] It may be conceivable that the TOF distributions measured in the PLD experiments could be contaminated by desorptions along the barrierless 4H pathway.[7] In order to avoid overestimation in evaluating mean translational energies $\langle E_{\mathrm{trans}}(\theta)\rangle$, which arises in the flux correction of fluctuating TOF density data,[1,2,7] the TOF curves were smoothed with two nonshifted Maxwellians characterized with temperatures of 1700 and 500 K, as shown in Fig. 1. After flux correction of the smoothed density curves, we evaluated $\langle E_{\mathrm{trans}}(\theta)\rangle=0.24\pm0.02$, 0.25 ± 0.02, and 0.26 ± 0.04 eV for $\theta=0°$, 20°, and 30°, respectively. The results were plotted in Fig. 2. It turns out that $\langle E_{\mathrm{trans}}\rangle$ is independent of θ within given error bars.

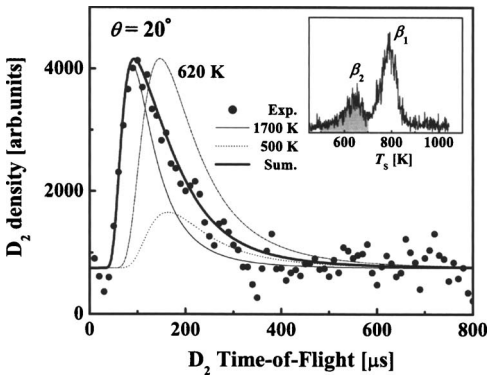

FIG. 1. TOF density spectra of D_2 molecules desorbing from the D(1.33 ML)/Si(100)-(3×1) surface for the desorption angle $\theta=20°$. The TOF density curve is fitted with two Maxwellian functions characterized with a 1700 K (dashed curve) and a 500 K (dotted curve) translational temperature. The thick solid line is the sum of the two components. Inset: the hatched part is the β_2-TPD spectrum for which TOF data were obtained.

In Fig. 3 we plot D_2 desorption yield as a function of θ. In addition to the yield data obtained from the TOF results, angular distributions obtained from the angle-resolved TPD spectra were also plotted. The experimental data can be best fitted with $\cos^m\theta$ for $m=2.3\pm0.3$ (not shown). We notice that the angular distribution of hydrogen molecules desorbed from the (3×1) dihydride phase is broader than that from the (2×1) monohydride phase where the sharper $\cos^m\theta$ function with $m\simeq5$ fits the data.[1,22] This difference of the desorption angular distributions observed in the two phases suggests that transition states for desorption are different among the two phases.

We invoke a microscopic reversibility of the desorption reaction from the dihydride phase, i.e., hydrogen molecules

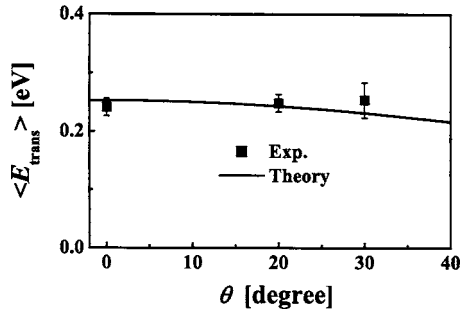

FIG. 2. Plots of mean translational energies $\langle E_{\mathrm{trans}}\rangle$ as a function of desorption angle θ. The solid line is the mean energies obtained by the theory on the basis of detailed balance for the predicted sticking coefficient as given in the text.

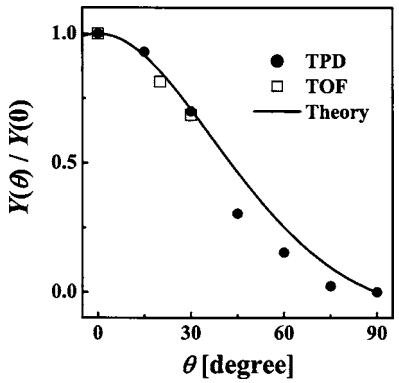

FIG. 3. Plots of angular distributions of D_2 desorption yield $Y(\theta)$ normalized at $\theta=0$. The solid line is the calculated angular distribution of desorption yields on the basis of detailed balance. The open and solid circles are the experimental data evaluated from the TOF distribution spectra and the angle-resolved TPD spectra, respectively.

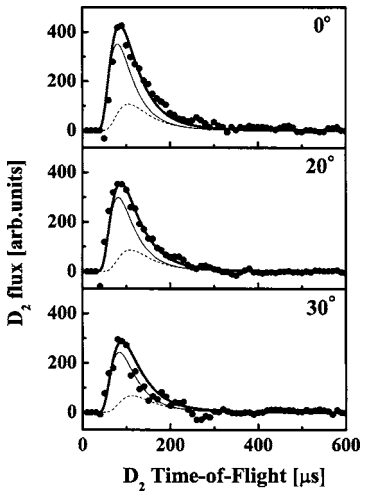

FIG. 4. Fits of the experimental TOF flux distributions with the theoretical TOF function obtained after applying detailed balance (see text).

can dissociatively stick onto the Si(100)-(2×1) monohydride surface. Applying detailed balance to the angle-dependent desorption dynamics shown in Figs. 1–3, sticking coefficients $s(E,\theta)$ for hydrogen adsorption onto the Si(100)-(2×1) monohydride surface are evaluated. To do this TOF flux distribution is expressed along the principle of detailed balance as a Maxwellian modified with $s(E,\theta)$,

$$f(t) \propto \frac{1}{t^5} \exp\{-M(L/t)^2/2kT_s\} s(M(L/t)^2/2,\theta)\cos\theta. \quad (2)$$

Here M is the mass of a D_2 molecule. We determine $s(E,\theta)$ by a curve-fitting method assuming an S-shaped sigmoid curve,

$$s(E,\theta) \propto \frac{1}{2}\left\{1+\tanh\left(\frac{E\cos^n\theta - E_0}{W}\right)\right\}, \quad (3)$$

where E_0 is the threshold energy at which s becomes a half of the saturated value, and W is the width of the curve. Here, the simple energy scaling for the effective energy available for adsorption, $E_{\text{eff}}(\theta)=E\cos^n\theta$, for the energy scaling parameter n, has been included to extract influence of the incidence angle to adsorption/desorption dynamics. For $n=2.0$ the surface is geometrically flat and the parallel momentum must be conserved during the reaction. In such a case, it can be anticipated that with increasing θ the more energy is necessary to overcome adsorption barriers. This would imply the more translational heating with the larger θ. For $0<n<2.0$ the surface is partially corrugated and the parallel energy can be fractionally available for the reaction. For $n=0$, on the other hand, the total incident energy is now available to overcome the barrier for adsorption. Hence, for the desorption dynamics predicted along the principle of detailed balance, $\langle E_{\text{trans}}(\theta)\rangle$ is expected to be independent of θ, provided that W is independent of θ.

In the actual curve-fitting process with trial and error analysis we found that two TOF components which are characterized with different sticking coefficients are necessary for the best fit: Referring the subscripts f and s to the fast and slow channels, respectively, we therefore express

$$s = C_f s_f + C_s s_s, \quad (4)$$

where C_f and C_s are the intensities of the fast and slow channels, respectively.

Since the observed TOF distribution shown in Fig. 1 exhibits considerable translational heating, the fast component must be the major desorption channel, while the slow one shares only a minor part of the desorption. In the actual curve fitting, it turned out that the most stringent parameters for the curve fit are W_f and n_f in s_f. The other parameter $E_{0,f}$ in s_f and all the parameters W_s, n_s, and $E_{0,s}$ in s_s are rather insensitive to the curve fit, giving rise to somewhat large error bars for those parameters. Taking $T_s=620$ K at around the TPD peak, the TOF curves can be best fitted with $s(E,\theta)$ for their parameters $E_{0,f}=2.0\pm1.0$ eV, $W_f=0.17\pm0.01$ eV, and $n_f=0.40\pm0.01$ for s_f, and $E_{0,s}=1.6\pm1.0$ eV, $W_s=0.3\pm0.1$ eV, and $n_s=2.0\pm1.0$ for s_s. The value of 2.0 eV for $E_{0,f}$ is agreeable with the theoretical result.[19] To show the fit quality we plot the best-fit TOF curves in Fig. 4 where one should remark that the density data plotted in Fig. 1 have been corrected to flux data after multiplying $1/t$. Using the same TOF flux functions Eq. (3), we calculate $\langle E_{\text{trans}}(\theta)\rangle$ and also $Y(\theta)$. The solid lines in Figs. 2 and 3 are the calculated results for $\langle E_{\text{trans}}(\theta)\rangle$ and also $Y(\theta)$, respectively. Notice that the experimental data are both consistently reproduced with the same TOF functions as determined above. This may further justify the above determined $s(E,\theta)$ functions. In Fig. 5 we plot $s(E,\theta)$ normalized with $s(\infty,\theta)$. One can notice that sticking of hydrogen onto the monohydride Si(100) surface is strongly activated by the incident translational energy E.

For $\theta=0°$ Eq. (3) predicts that the mean translational energy of the fast component is 0.29 eV$[T_t(=\langle E_{\text{trans}}\rangle/2k)=1740$ K], while for the slow one it gives 0.16 eV($T_t=990$ K). The yield ratio of the slow component to the fast one is 0.4 ± 0.1 at $\theta=0$, as plotted in Fig. 4, and it is almost unchanged with θ within the given error bar. The fast component could be attributed to the vibrationally ground $v=0$ molecules, while the slow one to the vibrationally excited $v=1$ molecules as measured in the REMPI experiments,[14,15] where the $v=1$ molecules were found to be overpopulated

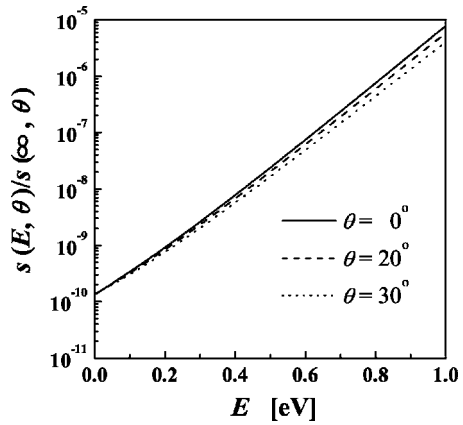

FIG. 5. Plots of normalized sticking coefficients $s(E,\theta)$ as a function of E for $\theta=0°$, 20°, and 30°.

beyond the equilibrium with mean vibrational energies of about 0.14 eV. However, we notice that the slow channel component appears to be nearly four times larger than the value evaluated in the REMPI experiment. This disagreement could be reconciled with a possible contamination of the present TOF spectra by the 4H and 3H channel desorptions from the monodeuteride units,[7] since they partially overlap with the β_2-TPD spectrum.

In Fig. 6 we propose a potential-energy curve for the adsorption of hydrogen onto the Si(100) monohydride phase or desorption from the dihydride phase. The energy barrier for adsorption on the monohydride surface is as high as 2 eV which should be compared with the ~1 eV adsorption barrier on the clean surface. As suggested by Vittadini and Selloni[19] this extremely high adsorption barrier may be resulted from an energy cost in breaking HSi–SiH dimer bonds. The molecules with $E(=\langle E_{\mathrm{trans}}\rangle)\simeq 0.25$ eV cannot break the Si–Si dimer bonds. Thus the barrier for adsorption must be mostly interacted by the substrate Si atoms bonded by the H adatoms rather than the molecules. To get to the

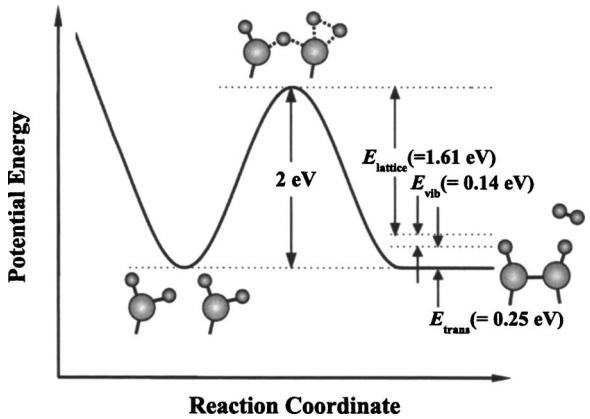

FIG. 6. Proposed potential-energy curve for the adsorption on the monohydride surface and desorption from the dihydride surface. The potential-energy curve is constructed from the parameters determined in the present work for $E_0=2.0$ eV and $E_{\mathrm{trans}}(=\langle E_{\mathrm{trans}}\rangle)=0.25$ eV, and also in the literatures of Refs. 14 and 15 for the mean molecular vibrational energy $E_{\mathrm{vib}}=0.14$ eV. The lattice energy, $E_{\mathrm{lattice}}=1.61$ eV, is the residual disposed by the 2 eV adsorption barrier. One should notice that it is close to the value of 1.65 eV reported by Vittadini and Selloni (Ref. 19). The canted structure of the locally (1×1) structure is taken from the literature (Refs. 18 and 19).

transition state for adsorption, one of the two H atoms on the doubly occupied Si dimers moves to a bridging position in between the two Si dimer atoms, elongating the Si–H bond. In this process the vibrational degrees of freedom of the Si–H bonds as well as the Si–Si dimer bonds play a key role, and the reaction is thus activated by the lattice thermal motions. At the same time, the sticking molecules also have to elongate their bond length at the transition state. This bond elongation may be achieved partly by a thermal excitation of the H–H vibrations in the gas phase and partly via translation-vibration energy conversion at the collision with the Si atom on which the H adatom has moved to the bridging position between the two Si atoms.

Desorption reaction may proceed just along the reversed path of this adsorption. One H atom of a pair of canted SiH_2 units shortens the Si–Si bond length to prepare the configuration suitable for the transition state, where the bond length of the two Si–H bonds on the counter SiH_2 unit is elongated. Desorption dynamics of the molecule is then determined as these two H adatoms make an elongated H–H bond at the transition state and start to slide along the potential-energy surface. The desorbing molecules will receive a Pauli repulsion from the Si back wall, and thus their center-of-mass motion is accelerated. Because of the large mass mismatch, the substrate Si atoms must be mostly static in nature during the passage of the molecules across the transition state region. Thus, the transition state configuration of the substrate Si atoms and H adatoms should have been prepared prior to the access of desorbing adatoms to the transition state for desorption. Hence, one can expect that the vibrational and translational motions of the molecules may be decoupled from the vibrational motion of the substrate atoms. This could be also the case for hydrogen desorption on the monohydride surface where the displacement of Si atoms is related to the Si dimer buckling. The dynamical decoupling of the motions of the substrate system and the desorbing molecules may result in such an apparently close similarity in the adsorption/desorption dynamics of hydrogen on both monohydride and dihydride surfaces, where the extent of translational and vibrational heating as well as the rotational cooling are found to be approximately the same. On the other hand, the extent of displacement of the Si atoms in the reaction is quite much different between the two surfaces: The breaking/bonding of the Si–Si dimer bonds during respective adsorption/desorption for dihydrides results in as large as 1.5 Å displacement of the Si atoms. On the other hand, for the monohydride surface the Si dimer buckling yields only a small displacement of the Si atoms. Therefore, the adsorption/desorption dynamics of hydrogen on the Si(100) surface manifests the feature characteristic to the so-called "phonon-assisted" reaction proposed by Brenig *et al.*[23] much more prominently in the dihydride phase than in the monohydride phase.

In summary, we measured polar angle (θ)-resolved time-of-flight spectra of D_2 molecules desorbed from the Si(100)-(3×1) dideuteride surface. The desorbed D_2 molecules exhibited a considerable translational heating with mean desorption kinetic energies of $\simeq 0.25$ eV, which was insensitive to the desorption angles for $0°\leqslant\theta\leqslant 30°$. The

observed angular distribution of desorbed molecules was much broader than that for the desorption from the monodeuteride phase.[2] The feature of desorption dynamics from the dideuteride phase is thus different from those from the monodeuteride phase, suggesting that the potential-energy surfaces along which the reaction dynamics is determined are different among the two phases. The desorption dynamics of D_2 from the dideuteride phase was discussed along the principle of detailed balance, and sticking coefficients of D_2 molecules onto the Si(100)-(2×1) monodeuteride surface were evaluated.

ACKNOWLEDGMENT

This work was financially supported by the grant-in-aid from the Ministry of Education, Science, Sport and Culture of Japan (Grant No. 17002011)

[1] T. Sagara, T. Kuga, K. Tanaka, T. Shibataka, T. Fujimoto, and A. Namiki, Phys. Rev. Lett. **89**, 086101 (2002).
[2] T. Shibataka, T. Matsuno, H. Tsurumaki, and A. Namiki, Phys. Rev. B **68**, 113307 (2003).
[3] M. Dürr, M. B. Raschke, and U. Höfer, J. Chem. Phys. **111**, 10411 (1999).
[4] M. Dürr and U. Höfer, Phys. Rev. Lett. **88**, 076107 (2002).
[5] A. Biedermann, E. Knoesel, Z. Hu, and T. F. Heinz, Phys. Rev. Lett. **83**, 1810 (1999).
[6] F. M. Zimmermann and X. Pan, Phys. Rev. Lett. **85**, 618 (2000).
[7] T. Matsuno, T. Niida, H. Tsurumaki, and A. Namiki, J. Chem. Phys. **122**, 024702 (2005).
[8] P. Gupta, V. L. Colvin, and S. M. George, Phys. Rev. B **37**, 8234 (1988).
[9] M. C. Flowers, N. B. H. Jonathan, Y. Liu, and A. Morris, J. Chem. Phys. **99**, 7038 (1993).
[10] U. Höfer, L. Li, and T. F. Heinz, Phys. Rev. B **45**, 9485 (1992).
[11] P. Nachtigall, K. D. Jordan, and C. Sosa, J. Chem. Phys. **101**, 8073 (1994).
[12] S. Ciraci and I. P. Batra, Surf. Sci. **178**, 80 (1986).
[13] S.-S. Ferng, C.-T. Lin, K.-M. Yang, D.-S. Lin, and T.-C. Chiang, Phys. Rev. Lett. **94**, 196103 (2005).
[14] K. W. Kolasinski, S. F. Shane, and R. N. Zare, J. Chem. Phys. **96**, 3995 (l992).
[15] S. F. Shane, K. W. Kolasinski, and R. N. Zare, J. Chem. Phys. **97**, 1520 (1992); S. F. Shane, K. W. Kolasinski, and R. N. Zare, J. Chem. Phys. **97**, 3704 (1992).
[16] K. W. Kolasinski, W. Nessler, A. de Meijere, and E. Hasselbrink, Phys. Rev. Lett. **72**, 1356 (1994).
[17] M. R. Radeke and E. A. Carter, Phys. Rev. B **55**, 4649 (1997).
[18] J. E. Northrup, Phys. Rev. B **44**, 1419 (1991).
[19] A. Vittadini and A. Selloni, Chem. Phys. Lett. **235**, 334 (1995).
[20] U. Freking, P. Krüger, A. Mazur, and J. Pollmann, Phys. Rev. B **69**, 035315 (2004).
[21] C. T. Rettner, H. M. Michelsen, and D. J. Auerbach, J. Chem. Phys. **102**, 4625 (1995).
[22] Y.-S. Park, J.-Y. Kim, and J. Lee, J. Chem. Phys. **98**, 757 (1993).
[23] W. Brenig, A. Gross, and R. Russ, Z. Phys. B: Condens. Matter **96**, 231 (1994).